

Impact of Na Doping on the Magnetic Characteristics of $\text{Zn}_{0.96-x}\text{Mn}_{0.04}\text{Na}_x\text{O}$ Substituted Nanocrystals (for $x = 0.02, 0.04$)

Bajrang Lal Prashant¹, Rajveer Singh², Savita Meena³

¹Department of Physics, A.R.S.D. College, University of Delhi, New Delhi, 110021, India
Corresponding Author Email: [bajranglal.prashant\[at\]gmail.com](mailto:bajranglal.prashant[at]gmail.com)

²Department of Physics, A.R.S.D. College, University of Delhi, New Delhi, 110021, India

³Department of Chemistry, M.S.J. Government P. G. College, Bharatpur, Rajasthan, 321001, India

Publication Date: 23 May 2024

Abstract: *Na co-doped ZnO: Mn, or $\text{Zn}_{0.96-x}\text{Mn}_{0.04}\text{Na}_x\text{O}$ nanoparticles, were synthesised using a wet chemical co-precipitation process with x ranging from 0.00 to 0.04 and are reported here. A superconducting quantum interference device (SQUID) was used to investigate the magnetic properties of the nanoparticles. Weak room-temperature ferromagnetism (RTFM) is observed in magnetisation experiments, and it becomes stronger as the Na concentration increases. There is a substantial link between the observed RTFM and oxygen vacancy defects produced by Na doping. To understand the fundamental mechanism of ferromagnetism in dilute magnetic semiconductor systems, the Na doping is correlated with the observable magnetic characteristics of the current system. Near-zero field data is shown in the insets, highlighting the samples' relative coercivity and remanence magnitudes. Furthermore, the magnetic moment increases with the rise in Na concentration from 2% to 4%, rising from 2.8 to 4.0 emu/g at 5 K.*

Keywords: ZnO, SQUID, Magnetisation, Oxygen vacancy

1. Introduction

The transition metal, because of their significance in basic study of physics and their exceptional applications in a variety of scientific and technological fields, such as charge and spin degrees of freedom that can be controlled by substituting magnetic ions for a small percentage of non-magnetic host semiconductor atoms, transition metal (TM) doped dilute magnetic semiconductors (DMSs), particularly the II–VI semiconductors, pique enormous interest in scientific research. Achieving ferromagnetism (FM) above room temperature (RT) is the primary obstacle to the practical use of these DMS materials, as it is incompatible with junction temperatures. Potential technical uses for these DMS materials include microwave devices, spintronics, magneto-electronics, and optoelectronics such as gas sensors, piezoelectric devices, transparent thin-film transistors, surface acoustic wave devices, and UV light-emitting diodes. [A.Wolf et. al. 2001, K.Yüksel et. al. 2013, Anurag P.C. et. al., 2014, Y. Köseoğlu et. al. 2014, and J.H. Li et. al. 2007].

Aspects of contemporary electronic gadgets [S.J. Pearton et. al.2003]. Mn-doped ZnO nanocrystals present a promising option for the development of transparent spintronics devices due to their visibility in the transparent region and the significant thermal equilibrium solubility of Mn in ZnO, which exceeds 10 mol% [T. Fukumura et. al. 1999]. For these reasons, Mn-doped ZnO nanocrystals have garnered considerable attention, leading to numerous studies. [A.S. Menon et. al. 2013, C. Jing et. al. 2010, X. Yan et. al. 2013, and C.O. Chey et. al. 2013].

The theoretical prediction of ferromagnetism has driven numerous experimental investigations into DMS

nanoparticles, employing a variety of synthesis techniques including heat processing, spray pyrolysis, mechanical milling, and organometallic synthesis from co-precipitation, sol-gel processes, microwave-assisted combustion, chemical precipitation, mechano-chemical synthesis, and hydrothermal methods. Researchers have focused on exploring the magnetic properties of TM-doped ZnO [D. Maouche et. al. 2007, R. Elilarassi et. al. 2010, Youming Zou et. al. 2010].

There is still disagreement on the genesis of ferromagnetism and the proper mechanism driving these magnetic behaviours of TM-doped oxides, despite a wealth of experimental data. According to controversial findings, pretreatment techniques have an impact on DMS magnetism. It has been demonstrated that the addition of TM dopants spreads carrier-mediated FM [S.J. Pearton et al., 2003; Y. Ohno et al., 1999; and J.M.D. Coey et. al. 2005] suggested donor impurity band exchange in DMS oxides, where shallow donor electrons generate bound magnetic polarons (BMP) that overlap to form a spin-split impurity band, mediating ferromagnetic exchanges.

There is disagreement about the involvement of both native defects and those caused by dopants or co-dopants, despite several theoretical models and justifications for the unusual nature of ZnO-type systems, including ferromagnetism, having been proposed. According to one widely accepted theory, the moment originates from native defects, such as interstitials or zinc vacancies, and the TM dopant functions as a charge reservoir, transferring electrons to the defect band or to nearby atoms that are charge deficient.

Apart from dopants, co-dopants—especially non-magnetic ones, such as Li, Na, or C — have a variety of roles. In general, they help improve how the TM charge transfers to

Volume 13 Issue 5, May 2024

Fully Refereed | Open Access | Double Blind Peer Reviewed Journal

www.ijsr.net

defects, creating favourable conditions for enhanced moments and potentially more mutual influence between neighbouring moment sites. Interesting outcomes have been obtained when groups of alkali metal elements, such as H, Li, and Na, are co-doped with Co ions in zinc oxide (ZnO). [J.M.D. Coey, et. al. 2008, M.H.F. Sluiter et. al. 2005, C.H. Park et. al. 2005, J.J. Li et. al. 2009, Y.H. Lin et. al. 2006, and H. Gu et. al. 2011].

A low-level integration of Li or Na may result in hole-related defects, which can cause minor ferromagnetism and p-type conductivity, according to a recent investigation of the substitution of first group elements alongside Mn in ZnO [Narendra Jakhar et al. 2018; L. Zhang et al. 2012]. Motivated by the publications mentioned earlier, we have examined the impact of Na co-doping in 4% Mn-doped ZnO on the magnetic characteristics of ZnO nanocrystals, contributing to the discussion on the genesis of ferromagnetism in TM-doped ZnO nanocrystals. Important discoveries about Na-doped ZnO nanoparticles, a first-group element, served as the impetus for our investigation [B. Karthikeyan et al. 2012].

According to the findings, oxygen vacancy problems are caused by Na doping. Defect production occurs when Li is added to the $\text{Zn}_{0.96}\text{Mn}_{0.04}\text{O}$ lattice, as indicated by the PAS investigation, and the defect density increases with rising Li concentration [Narendra Jakhar et al., 2018]. When Na is substituted for the divalent Zn cation, the total cationic valence state is decreased since Na is a monovalent (+1) cation from the first group. Defects at the anion (oxygen) site and/or electrical charge transfer may result from this modification. To gain a better understanding of the mechanism of ferromagnetism in these doped Dilute magnetic semiconductor systems, it is interesting to examine how electronic processes, such as charge transfer and defect formation, affect the magnetic characteristics of ZnO and Mn.

Using a low-temperature wet chemical co-precipitation approach, we created nanocrystalline samples of $\text{Zn}_{0.96-x}\text{Mn}_{0.04}\text{Na}_x\text{O}$ with $x = 0.02, 0.03$, and 0.04 . We also used a SQUID to test the magnetism at ambient temperature and 5 K.

2. Experimental Details

2.1 Sample preparation

Low-temperature wet chemical co-precipitation was used to create the Na co-doped ZnO: Mn ($\text{Zn}_{0.96-x}\text{Mn}_{0.04}\text{Na}_x\text{O}$) series of nanocrystalline samples with x values of 0.02 and 0.04. The precursor materials were analytical-grade sodium acetate ($\text{Na}(\text{CH}_3\text{COO}) \cdot 2\text{H}_2\text{O}$), manganese acetate ($\text{Mn}(\text{CH}_3\text{COO})_2 \cdot 4\text{H}_2\text{O}$), and zinc acetate ($\text{Zn}(\text{CH}_3\text{COO})_2 \cdot 2\text{H}_2\text{O}$). KOH was employed as the precipitating agent in molar solutions of these acetates, which were made in distilled water. The mixture was allowed to cool to ambient temperature after being progressively heated to approximately 60°C , while maintaining a pH of 11. To remove CH_3COOK , the resultant precipitates were carefully washed with water. After further cleaning the samples with

acetone and ethyl alcohol, the powder was annealed in air at 400°C to produce dry nanoparticles.

2.2 Magnetisation measurements

With the aid of a superconducting quantum interference device (SQUID) magnetometer, field-dependent magnetisation measurements and the overall magnetic behaviour of the sample at room temperature have been examined. These measurements were conducted in the field up to 7 kOe and in the temperature range $5\text{ K} < T < 300\text{ K}$. An electromagnet and a closed-cycle refrigerator cryostat (CCR) were employed. We first recorded the magnetic moment v/s field at ambient temperature for the M-H measurements. Next, we cooled the sample to zero field and set the temperature to 5 K. Finally, we recorded the magnetic moment versus field at 5 K once again.

3. Results and Discussion

The magnetic hysteresis curves for $\text{Zn}_{0.96-x}\text{Mn}_{0.04}\text{Na}_x\text{O}$ nanoparticles with $x = 0.02$ and 0.04 recorded at 300 K and 5 K are displayed in Figures 1 and 2 using a superconducting quantum interference device. The pure ZnO sample exhibits diamagnetic behaviour [R.K. Singhal et al. 2009]. However, Figure 1 300 K hysteresis curves reveal a mild ferromagnetic alignment at normal temperature inside the $\text{Zn}_{0.96-x}\text{Mn}_{0.04}\text{Na}_x\text{O}$ nanocrystalline structure samples, where $x = 0.02$ and 0.04 at 300 K. The hysteresis loops' form did not wholly rule out the potential of a paramagnetic (PM) contribution in the samples; nevertheless, when the temperature was lowered to 5K, the PM impact decreased.

Near-zero field data is shown in the insets, highlighting the samples' relative coercivity and remanence magnitudes. Furthermore, the magnetic moment increases with the Na concentration from 2% to 4% (see Figure 2), rising from 2.8 to 4.0 emu/g at 5 K.

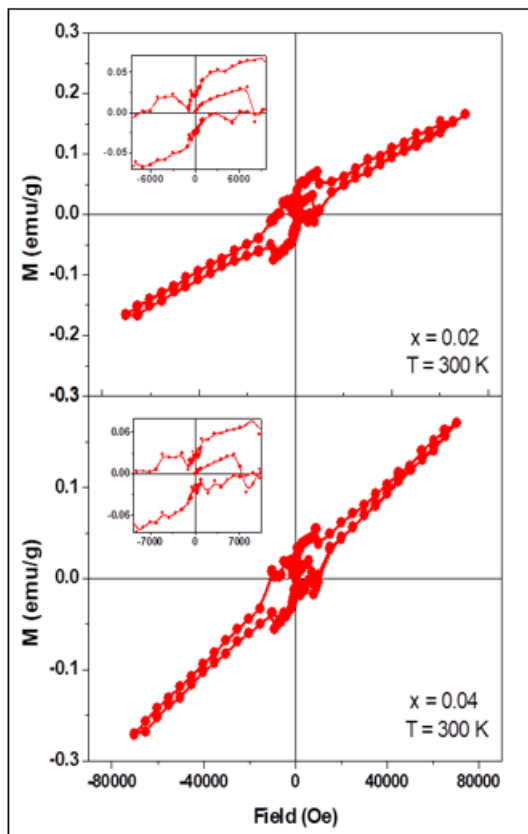


Figure 1: M-H Measurement made in the Field up to 7 Tesla at 300 K

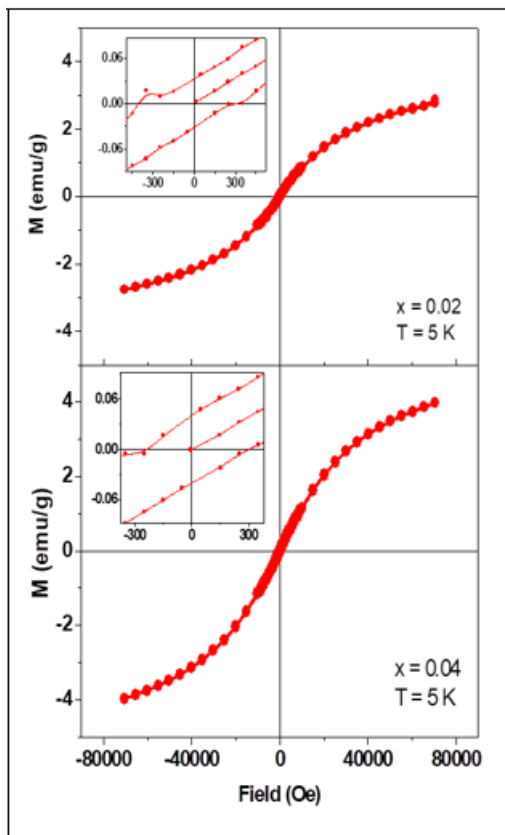


Figure 2: M-H Measurement made in the Field up to 7 Tesla at 5 K

4. Conclusion

Using a wet chemical co-precipitation approach, we have effectively produced $\text{Zn}_{0.96-x}\text{Mn}_{0.04}\text{Na}_x\text{O}$ nanoparticles with x values of 0.02 and 0.04. Weak room-temperature ferromagnetism is well demonstrated by SQUID magnetisation experiments, and it becomes stronger as the Na concentration rises. A substantial link exists between the observed ferromagnetism and oxygen vacancy defects, which are likely caused by Na doping. This correlation advances our understanding of the ferromagnetism process in diluted magnetic semiconductors. It highlights the role that Na doping plays in influencing the system's magnetic properties, as evident in the relative magnitudes of coercivity and remanence in the samples. The magnetic moment increases with increasing Na concentration from 2% to 4%, rising from 2.8 to 4.0 emu/g at 5 K.

References

- [1] Narendra Jakhar, Naresh Chejara, R.K. Singhal, S.N. Dolia, S.K.Gupta,H.S. Palsania B L Prashant, IEEE (2018).
- [2] A. Wolf, D.D. Awschalom, R.A. Buhrman, J.M. Daughton, S. von Molnar, M.L. Roukes, A.Y. Chtchelkanova, D. M. Treger, Science 294 (2001) 1488.
- [3] A.S. Menon, N. Kalarikkal, S. Thomas, Indian J. NanoSci. 1 (2013) 16.
- [4] Anurag Prakash Chand,Gaur, Ashavani Kumar, J. Alloys Compd. 585 (2014) 345.
- [5] B. Karthikeyan, C.S. Sandeep, T. Pandiyarajan, P. Venkatesan and R. Philip, Appl. Phys. Lett. 95 (2012) 023118.
- [6] C.H. Park and D.J. Chadi, Phys. Rev. Lett. 94 (2005) 127204.
- [7] C.O. Chey, O. Nur, M. Willander, J. Cryst. Growth 375 (2013) 125.
- [8] D. Maouche, P.Ruterana, L.Louail, Phys. Lett. A 365 (2007) 231–234.
- [9] H. Gu, Y. Jiang, Y.B. Xu and M. Yan, Appl. Phys. Lett. 98 (2011) 012502.
- [10] J.H. Li, D.Z. Shen, J.Y. Zhang, D.X. Zhao, B.S. Li, Y.M. Lu, Y.C. Liu, X.W. Fan, J. Lumin. 122 (2007) 352
- [11] J.J. Li, W.C. Hao, H.Z. Xu, T.M. Wang and J. Shi, J. Appl. Phys. 106 (2009) 063915.
- [12] J.M.D. Coey, K. Wongsaprom, J. Alaria and M. Venkatesan, J. Phys. D: Appl. Phys. 41 (2008)134012.
- [13] J.M.D. Coey, M. Venkatesan, C.B. Fitzgerald, Nature Materials 4 (2005) 173.
- [14] L. Zhang, Y. Zhang, Z. Ye, J. Lu, B. Lu, and B. He, J. Appl. Phys. 111 (2012) 123524.
- [15] M.H.F. Sluiter, P. Sharma, A. Inoue, A.R. Raju, C. Rout C and U.V. Waghmare, Phys. Rev. Lett. 94 (2005) 187204.
- [16] R. Elilarassi, G. Chandrasekaran, Mater. Chem. Phys. 123 (2010) 450.
- [17] S.J. Pearton, C.R. Abernathy, M.E. Overberg, G.T. Thaler, D.P.Norton, N. Theodoropoulou, A.F. Hebard, Y.D. Park, F. Ren, J. Kim, L.A. Boatner, J. Appl. Phys. 93 (2003)1.

- [18] T. Fukumura, Z. Jin, A. Ohtomo, H. Koinuma, M. Kawasaki, Appl. Phys. Lett. 75 (1999) 3366.
- [19] X. Yan, T. Itoh, S. Dai, Y. Ozaki, Y. Fang, J. Phys. Chem. Solids 74(2013) 1127.
- [20] Y. Ohno, D.K. Young, B. Beshoten, F. Matsukura, H. Ohno, D.I. Awschalom, Nature 402 (1999) 790.
- [21] Y.H. Lin, J. Cai, C.W. Nan, M. Kobayashi and J. He, J. Appl. Phys. 99 (2006) 056107.
- [22] Y. Köseoğlu, Ceram. Int. 40 (2014) 4673.
- [23] Youming Zou, Zhe Qu, Jun Fang, Yuheng Zhang, J. Magn. Magn. Mater. 321 (2010) 3352.
- [24] Yüksel Köseoğlu, J. Supercond. Novel Magn. 26 (2013) 485.